FIG. 2. The number of the multinucleated giant cells was counted. The nuclei in all of the multinucleated cells with five nuclei or more were counted. The average number of nuclei was significantly higher in the RA group. $*P < 0.05$ *vs* OA.

multinucleated cells were induced by those cytokines in a dose-dependent manner and then the effect became fixed both in RA and OA.

Number of resorption pits on the dentin slices, and the percentage resorption on Osteologic discs

In order to determine the ability of multinucleated cells to absorb bone, the CD14-positive monocyte-like cells were cultured in

medium with IL-3 for 14 days on either dentin slices or Osteologic discs. After the incubation period, the multinucleated giant cells from CD14-positive monocyte-like cells in the IL-3-stimulated RA-SF and OA-SF samples formed resorption pits on the dentin slices. The number of resorption pits formed by the RA-SF was significantly higher (143.0 ± 19.52; $P < 0.05$) than that formed by the OA-SF (9.0 ± 2.0) (Fig. 7). Since all of the cultures formed resorption pits on the Osteologic discs, the percentage resorption was calculated as the area of resorption relative to the total surface area of the disc. A marked increase in lacunar resorption was noted for the RA-SF cultures, in which the extent of resorption was $46.04 \pm 6.39\%$, as compared with that of the OA-SF cultures ($12.38 \pm 2.18\%$; $P < 0.05$) (Fig. 8). When the CD14-positive cells were purified from RA-SF and OA-SF which does not pre-culture for 4 weeks, they did not form resorption pits on either dentin slices or Osteologic discs (data not shown).

Discussion

In this study, we demonstrated that multinucleated bone-resorbing giant cells were induced from CD14-positive monocyte-like cells in both RA-SF and OA-SF. However, the fusion indices and functional parameters of multinucleated cells that were derived from CD14-positive monocyte-like cells were increased in the RA-SF. While the percentages of monocyte/macrophage cells were similar, the absolute numbers of those cells were significantly higher in RA-SF than in OA-SF. These results suggest that the RA-SF contains many more cells with the ability to differentiate into TRAP-positive preosteoclasts than are found in the OA-SF. The resorption pits on either dentin slices or Osteologic discs of multinucleated cells that were derived from CD14-positive
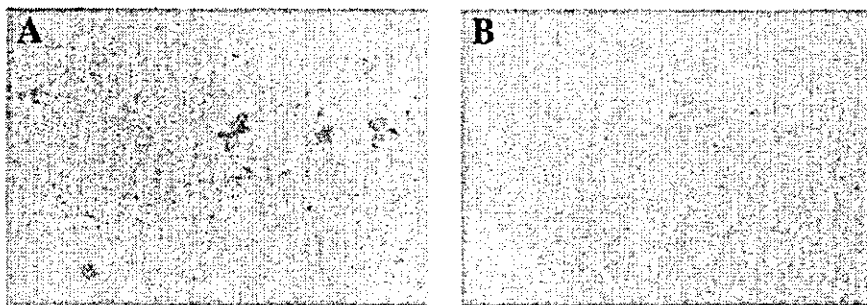

FIG. 3. Examination of resorption pits formed by multinucleated bone-resorbing giant cells on dentin slices. The CD14-positive monocyte-like cells were cultured with IL-3 (1 ng/ml) for 14 days on dentin slices. (A) Resorption pits were observed on dentin slices by bone-resorbing giant cells which were derived from CD14-positive cells from the RA-SF, but (B) not observed from the OA-SF. Original magnification ×200.
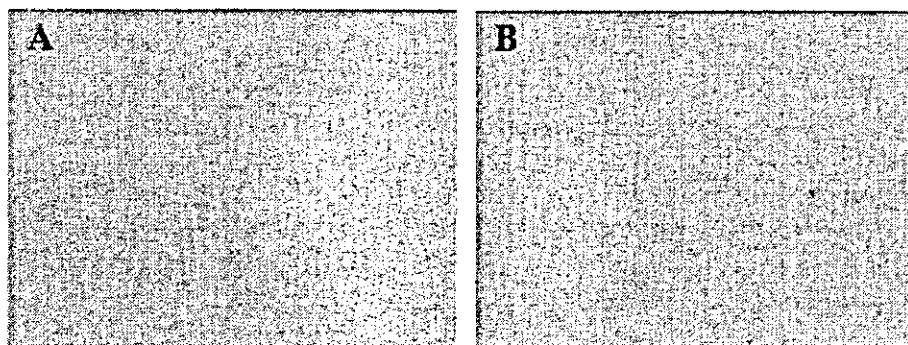

FIG. 4. Examination of resorption area formed by multinucleated bone-resorbing giant cells on Osteologic discs by using phase-contrast microscopy. The CD14-positive monocyte-like cells were cultured with IL-3 (1 ng/ml) for 14 days on Osteologic discs. (A) A wide-ranging area was formed by bone-resorbing giant cells which were derived from CD14-positive cells from the RA-SF, but (B) not formed in OA-SF. Original magnification ×100.
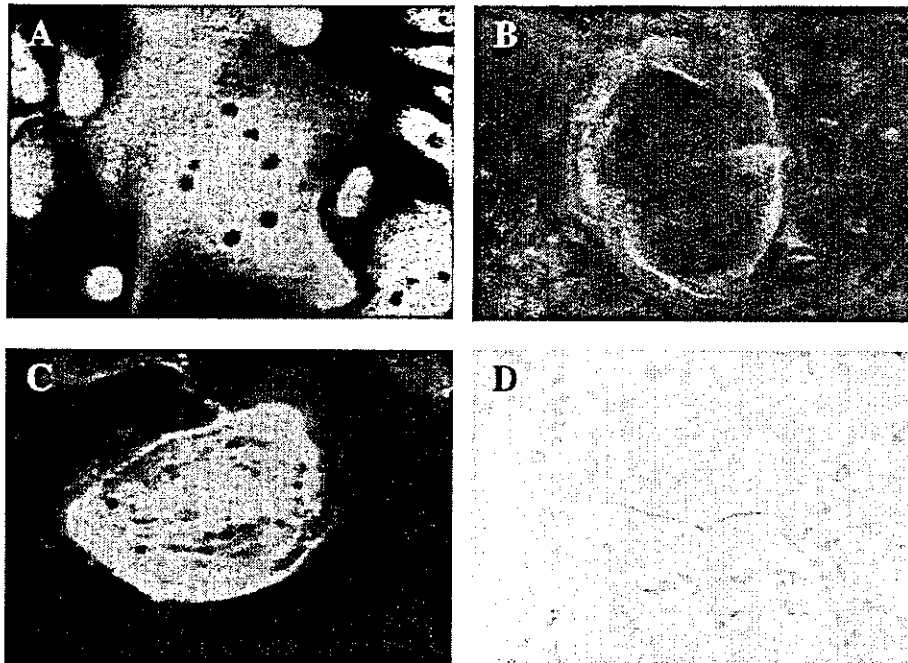
FIG. 5. Immunocytochemical examination of multinucleated giant cells which were derived from CD14-positive cells from the RA-SF. The CD14-positive monocyte-like cells were cultured with IL-3 (1 ng/ml). Multinucleated giant cells were positive for (A) carbonic anhydrase II, (B) actin, (C) vitronectin receptor, (D) calcitonin receptor. Original magnification ×200.
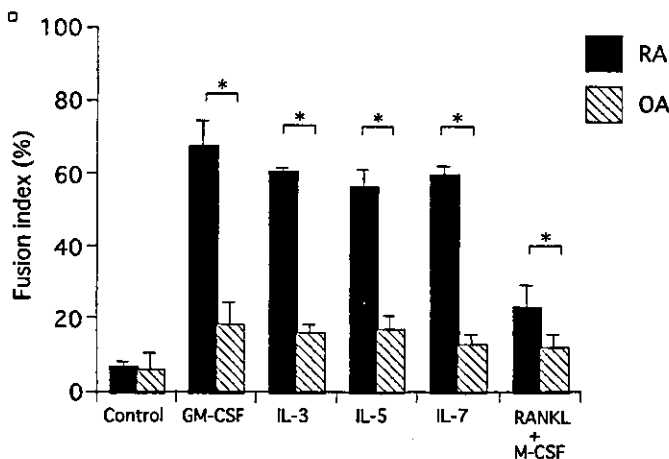

FIG. 6. IL-3, IL-5, IL-7, GM-CSF and a combination of RANKL and M-CSF induced the differentiation of CD14-positive monocyte-like cells into multinucleated cells. *$P < 0.05$ vs OA.
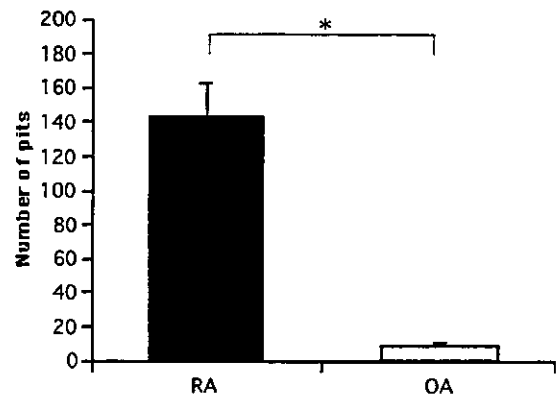

FIG. 7. Comparison of capability of resorption pit formation on dentin slices between bone-resorbing giant cells which were derived from CD14-positive cells from the RA-SF and OA-SF. The number of resorption pits was counted under microscopic examination. The number of resorption pits formed by the RA-SF was significantly higher than that formed by the OA-SF. *$P < 0.05$ vs OA.

monocyte-like cells were increased in the RA-SF. In these functional parameters, high bone-resorbing activity of multinucleated cells in the RA-SF may be related to the survival rate or the number of multinucleated cells.

We reported previously that CD14-positive monocyte-like cells could be induced and maintained in the presence of nurse-like cells (RA-NLC), which were isolated from RA synovial tissue and bone marrow [32]. These cells expressed TRAP activity, and differentiated into multinucleated bone-resorbing giant cells when stimulated with IL-3, IL-5, IL-7 or GM-CSF in the absence of accessory cells. The RA-NLCs were shown to play an important role in the differentiation and maturation of lymphocytes through pseudoemperipolesis in RA joints [29–31]. In the primary cultures of SF mononuclear cells, the relatively large, round-shaped, non-adherent cells and adherent cells predominated after 3 weeks, and some of these adherent cells had nursing activities (H. Takano, personal communication), which suggests that adherent cells with

nursing activities may play a role in the osteoclastogenesis observed in this study.

The multinucleated bone-resorbing cells shown in this study differentiated in the presence of IL-3, IL-5, IL-7 and GM-CSF. These cytokines and growth factors are known to promote the proliferation and differentiation of primitive haematopoietic cells. IL-3, IL-5 and GM-CSF are produced by activated T cells, and their receptors contain a common beta subunit [36]. In the present study, we found that CD4-positivity was more prevalent in the RA-SF than in the OA-SF, which suggests that T cells accumulate and produce IL-3, IL-5 and GM-CSF in the RA synovial fluid. GM-CSF is often detected in the joints of RA patients [37, 38], and synovial RA-NLCs produce GM-CSF in vitro [29, 30]. Matayoshi et al. [3] reported that both IL-3 and GM-CSF induced the differentiation of haematopoietic precursor cells into osteoclasts in the absence of stromal cells [3].
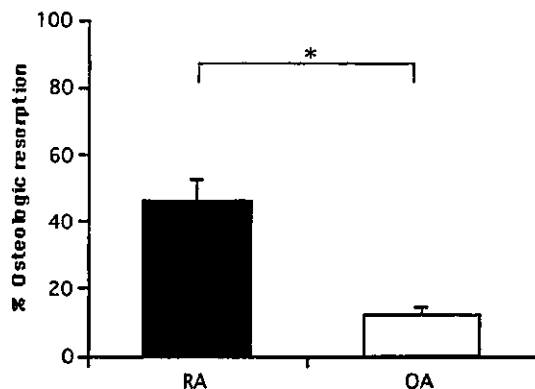
H. Takano *et al.*

FIG. 8. Comparison of capability of resorbing area on Osteologic discs between bone-resorbing giant cells which were derived from CD14-positive cells from the RA-SF and OA-SF. The resorbed area on each disc was measured using the MacSCOPE image analyser. A marked increase in lacunar resorption was noted for the RA-SF cultures as compared with that of the OA-SF cultures. $*P<0.05$ *vs* OA.

RANKL has been reported as a potent inducer of osteoclast development from monocytes, and is a key molecule in osteoclastogenesis [39, 40]. However, it was very interesting to note that a mixture of RANKL and M-CSF exhibited weaker induction of multinucleated cells than IL-3, IL-5, IL-7 and GM-CSF in our experiments. This finding suggests that stimulation of IL-3, IL-5, IL-7 and GM-CSF at the step of fusion of the pre-cultured CD14-positive monocyte-like cells is more dominant than RANKL. However, it is likely that RANKL is participating in differentiation of CD14-positive monocyte-like cells into preosteoclasts during the co-culture with fibroblast-like cells.

In this study, the fusion indices and functional parameters of the multinucleated cells, which were derived from CD14-positive monocyte-like cells, were much higher in the RA-SF than in the OA-SF. This result concurs with the conclusions of previous reports, in which histochemical studies indicated that TRAP-positive multinucleated cells were more numerous in the RA synovium than in the OA synovium [21, 41, 42]. In this study, similar numbers of CD14-positive cells were cultured from the SF of RA and OA patients, but there were significant differences between the RA-SF and OA-SF in terms of fusion indices and bone resorption activities. Our results suggest that the functions of CD14-positive cells may be enhanced in RA due to the enhanced ability of RA-SF stromal cells with nursing activity to support the differentiation of monocyte-like cells into TRAP-positive preosteoclasts. A detailed investigation of the differences in CD14-positive cell populations between RA and OA patients is underway.

In conclusion, CD14-positive cells and activated T cells in the RA-SF may play important roles in RA pathogenesis, which is characterized by progressive bone destruction and the enhanced function of haematopoietic cells, such as preosteoclast-like cells. These discoveries may provide a tool for understanding the mechanisms of bone destruction in RA, and for the development of effective treatments for joint destruction in RA patients.

References

1. Athanasou NA. Cellular biology of bone resorbing cells. J Bone Joint Surg 1996;78A:1096–112.
2. Akagawa KS, Takatsuka N, Nozaki Y *et al.* Generation of CD1+ RelB+ dendritic cells and tartrate-resistant acid phosphatase-positive osteoclast-like multinucleated giant cells from human monocytes. Blood 1996;88:4029–39.
3. Matayoshi A, Brown C, DiPersio JF *et al.* Human blood-mobilized hematopoietic precursors differentiate into osteoclasts in the absence of stromal cells. Proc Natl Acad Sci USA 1996;93:10785–90.
4. Bromley M, Woolley DE. Chondroclasts and osteoclasts at subchondral sites of erosion in the rheumatoid joint. Arthritis Rheum 1984;27:968–75.
5. Hagenaars CE, Van der Kraan AA, Kawilarang-de Haas EW, Visser JW, Nijweide PJ. Osteoclast formation from cloned pluripotent hemopoietic stem cells. Bone Miner 1989;6:179–89.
6. Sheven BA, Viser JW, Nijweide PJ. *In vitro* osteoclast generation from different bone marrow fractions, including a highly enriched haematopoietic stem cell population. Nature 1986;321:79–81.
7. Suda T, Takahashi N, Martin TJ. Modulation of osteoclast differentiation. Endocr Rev 1992;13:66–80.
8. Takahashi N, Udagawa N, Akatsu T, Tanaka H, Isogai Y, Suda T. Deficiency of osteoclasts in osteoporotic mice is due to a defect in the local microenvironment provided by osteoblastic cells. Endocrinology 1991;128:1792–6.
9. Tamura T, Udagawa N, Takahashi N *et al.* Soluble interleukin-6 receptor triggers osteoclast formation by interleukin-6. Proc Natl Acad Sci USA 1993;90:11924–8.
10. Yasuda H, Shima N, Nakagawa N *et al.* Osteoclast differentiation factor is a ligand for osteoprotegerin/osteoclastogenesis-inhibitory factor and is identical to TRANCE/RANKL. Proc Natl Acad Sci USA 1998;95:3597–602.
11. Takayanagi H, Oda H, Yamamoto S *et al.* A new mechanism of bone destruction in rheumatoid arthritis: synovial fibroblasts induce osteoclastogenesis. Biochem Biophys Res Commun 1997;240:279–86.
12. Fujikawa Y, Shingu M, Torisu T, Itonaga I, Masumi S. Bone resorption by tartrate-resistant acid phosphatase-positive multinuclear cells isolated from rheumatoid synovium. Br J Rheumatol 1996;35:213–7.
13. Fujikawa Y, Sabokbar A, Nealev S, Athanasou NA. Human osteoclast formation by monocytes and synovial macrophages in rheumatoid arthritis. Ann Rheum Dis 1996;55:816–22.
14. Fontana A, Hengartner H, Weber E, Fehr K, Grob PJ, Cohen G. Interleukin 1 activity in the synovial fluid of patients with rheumatoid arthritis. Rheumatol Int 1982;2:49–53.
15. Wood DD, Ihrie EJ, Dinarello CA, Cohen PL. Isolation of an interleukin-1-like factor from human joint effusions. Arthritis Rheum 1983;26:975–83.
16. Nouri AM, Panayi GS, Goodman SM. Cytokines and the chronic inflammation of rheumatic disease. I. The presence of interleukin-1 in synovial fluids. Clin Exp Immunol 1984;55:295–302.
17. Miossec P, Dinarello CA, Ziff M. Interleukin-1 lymphocyte chemotactic activity in rheumatoid arthritis synovial fluid. Arthritis Rheum 1986;29:461–70.
18. Saxne T, Palladino MA Jr, Heinegard D, Talal N, Wollheim FA. Detection of tumor necrosis factor alpha but not tumor necrosis factor beta in rheumatoid arthritis synovial fluid and serum. Arthritis Rheum 1988;31:1041–5.
19. Hirano T, Matsuda T, Turner M *et al.* Excessive production of interleukin 6/B cell stimulatory factor-2 in rheumatoid arthritis. Eur J Immunol 1988;18:1797–801.
20. Guerne PA, Zuraw BL, Vaughan JH, Carson DA, Lotz M. Synovium as a source of interleukin 6 *in vitro*. Contribution to local and systemic manifestations of arthritis. J Clin Invest 1989;83:585–92.
21. Kotake S, Sato K, Kim KJ *et al.* Interleukin-6 and soluble interleukin-6 receptors in the synovial fluids from rheumatoid arthritis patients

are responsible for osteoclast-like cell formation. J Bone Miner Res 1996;11:88–95.

22. Kotake S, Udagawa N, Takahashi N et al. IL-17 in synovial fluids from patients with rheumatoid arthritis is a potent stimulator of osteoclastogenesis. J Clin Invest 1999;103:1345–52.

23. Manabe N, Oda H, Nakamura K, Kuga Y, Uchida S, Kawaguchi H. Involvement of fibroblast growth factor-2 in joint destruction of rheumatoid arthritis patients. Rheumatology 1999;38:714–20.

24. Wekerle H, Ketelsen UP, Ernst M. Thymic nurse cells: Lymphoepithelial cell complexes in murine thymuses: morphological and serological characterization. J Exp Med 1980;151:925–44.

25. Wekerle H, Ketelsen UP. Thymic nurse cells: Ia-bearing epithelium involved in T-lymphocyte differentiation? Nature 1980;283:402–4.

26. Brelinska R, Seidel HJ, Kreja L. Thymic nurse cells: differentiation of thymocytes within complexes. Cell Tissue Res 1991;264:175–83.

27. Pezzano M, Li Y, Philp D, Omene C, Cantey M, Saunders G. Thymic nurse cell rescue of early CD4+ CD8+ thymocytes from apoptosis. Cell Mol Biol (Noisy-le-grand) 1995;41:1099–111.

28. Hiramine C, Nakagawa T, Miyauchi A, Hojo K. Thymic nurse cells as the site of thymocyte apoptosis and apoptotic cell clearance in the thymus of cyclophosphamide-treated mice. Lab Invest 1996;75:185–201.

29. Takeuchi E, Tomita T, Toyosaki-maeda T et al. Establishment and characterization of nurse cell-like stromal cell lines from synovial tissue of patients with rheumatoid arthritis. Arthritis Rheum 1999;42:221–8.

30. Tomita T, Takeuchi E, Toyosaki-maeda T et al. Establishment of nurse cell-like stromal cells from bone marrow of patients with rheumatoid arthritis: indication of characteristic bone marrow microenvironment in patients with rheumatoid arthritis. Rheumatology 1999;38:854–63.

31. Shimaoka Y, Attrep JF, Hirano T et al. Nurse-like cells from bone marrow and synovium of patients with rheumatoid arthritis promote survival and enhance function of human B cells. J Clin Invest 1998;102:606–18.

32. Toyosaki-Maeda T, Takano H, Tomita T et al. Differentiation of monocytes into multinucleated giant bone-resorbing cells: two-step differentiation induced by nurse-like cells and cytokines. Arthritis Res 2001;3:306–10.

33. Arnett FC, Edworthy SM, Bloch DA et al. The American Rheumatism Association 1987 revised criteria for the classification of rheumatoid arthritis. Arthritis Rheum 1988;31:315–24.

34. Higuchi S, Tabata N, Tajima M et al. Induction of human osteoclast-like cells by treatment of blood monocytes with anti-fusion regulatory protein-1/CD98 monoclonal antibodies. J Bone Miner Res 1998;13:44–9.

35. Toyosaki T, Tsuruta Y, Yoshioka T et al. Recognition of rheumatoid arthritis synovial antigen by CD4+, CD8– T cell clones established from rheumatoid arthritis joints. Arthritis Rheum 1988;41:92–100.

36. Kitamura T, Sato N, Arai K, Miyajima A. Expression cloning of the human IL-3 receptor cDNA reveals a shared beta subunit for the human IL-3 and GM-CSF receptors. Cell 1991;66:1165–74.

37. Chu CQ, Field M, Allard S, Abney E, Feldmann M, Maini RN. Detection of cytokines at the cartilage/pannus junction in patients with rheumatoid arthritis: implications for the role of cytokines in cartilage destruction and repair. Br J Rheumatol 1992;31:653–61.

38. Bell AL, Magill KK, McKane WR, Kirk F, Irvine AE. Measurement of colony-stimulating factors in synovial fluid: potential clinical value. Rheumatol Int 1995;14:177–82.

39. Lacey DL, Timms E, Tan HL et al. Osteoprotegerin ligand is a cytokine that regulates osteoclast differentiation and activation. Cell 1998;17:165–76.

40. Kong YY, Yoshida H, Sarosi I et al. OPGL is a key regulator of osteoclastogenesis, lymphocyte development and lymph-node organogenesis. Nature 1999;28:315–23.

41. Ashton BA, Ashton IK, Marshall MJ, Butler RC. Localization of vitronectin receptor immunoreactivity and tartrate resistant acid phosphatase activity in synovium from patients with inflammatory or degenerative arthritis. Ann Rheum Dis 1993;52:133–7.

42. Suzuki Y, Tsutsumi Y, Nakagawa M et al. Osteoclast-like cells in an in vitro model of bone destruction by rheumatoid synovium. Rheumatology 2001;40:673–82.

Evidence for existence of oligoclonal tumor-infiltrating lymphocytes and predominant production of T helper 1/T cytotoxic 1 type cytokines in gastric and colorectal tumors

TAKAJI MATSUTANI[1,2], KEN-ICHI SHIIBA[3], TAKESHI YOSHIOKA[2], YUJI TSURUTA[2], RYUJI SUZUKI[2,4], TAKAHIRO OCHI[4], TSUNETOSHI ITOH[1], HIROAKI MUSHA[3], TAKAYUKI MIZOI[3] and IWAO SASAKI[3]

[1]Division of Immunology and Embryology, Department of Cell Biology, Tohoku University School of Medicine, Sendai; [2]Discovery Research Laboratories, Shionogi Research Laboratories, Shionogi and Co., Ltd., Osaka; [3]Division of Biological Regulation and Oncology, Department of Surgery, Tohoku University Graduate School of Medicine, Sendai; [4]Department of Rheumatology and Clinical Immunology, Clinical Research Center for Rheumatology and Allergy, National Sagamihara Hospital, Kanagawa, Japan

Abstract. Tumor-infiltrating lymphocytes (TIL) play a central role in cellular immunity against tumor. We have revealed the characteristics of TILs in terms of T-cell receptor (TCR) repertoire, T-cell clonality, and cytokine production. TCR repertoire analyses and CDR3 size spectratyping were performed using peripheral blood mononuclear cells (PBMCs) and tissue specimens of gastric or colorectal cancers surgically resected from 11 patients. The cytokine expression was measured by real-time quantitative polymerase chain reaction. TCR repertoires were similar among multiple tissue specimens from different sites of the same tumor. Similar peak patterns of CDR3 size spectratyping were observed among these tumor specimens, but not in normal tissues or PBMCs. In addition, identical peaks were detected in multiple specimens of the same tumor. The ratio of the levels of IFN-γ to that of IL-4 is significantly higher for tumor lesions compared with PBMCs. These results suggested that a limited number of TILs locally expand in response to tumor antigens exiting within gastric or colorectal cancers and local predominant production of the T helper 1/T cytotoxic 1 type cytokine may affect the anti-tumor immune response of TILs.

Introduction

The host immune system recognizes tumor cells and tries to reject tumors such as melanoma. In the anti-tumor

Correspondence to: Dr Takaji Matsutani, Division of Immunology and Embryology, Department of Cell Biology, Tohoku University School of Medicine, 2-1 Seiryo-machi, Aoba-ku, Sendai 980-8575, Japan

E-mail: matsu@immem.med.tohoku.ac.jp

response, tumor-infiltrating T lymphocytes (TIL) are known to play a significant role (1). TILs are enriched with T-cells, which recognize antigens expressed on the surface of autologous tumor cells (2). Differential antigens such as Melan-A/MART-1 (3-5), tumor-associated antigens (6) or mutated self-antigens (7) have been defined as tumor-specific antigens. These antigens or antigen peptides specific for tumors have been developed for cancer vaccines, which can induce anti-tumor-specific T-cells. Many approaches to therapeutic cancer vaccine development have been under clinical trial.

In many human cancers other than melanoma, the anti-tumor response mediated by T-cells occurs in limited local sites around the tumor, although the immune response in no way controls tumor growth. Gaudin *et al* has already described local expansion of T-cell clones in renal cell carcinoma (8). However, little is known about whether TILs respond to tumor antigens in patients with gastric or colorectal cancer and what the functional characteristics of the TILs are. Proliferation of T-cells specific for tumor antigens can skew TCR repertoires in local sites around the tumor. Determination of the usage of TCR repertoires at local sites allows us to demonstrate that the existence of TILs that can exert an anti-tumor immune response and enable us to clarify the characteristics of TILs. T-cells recognize a peptide antigen present on the surface of a major histocompatibility antigen (MHC) molecule (9). Therefore, TILs that recognize a common antigen are thought to express the same or a similar T-cell receptor. Analysis of the specific T-cell receptor (TCR) of TIL can provide information on the nature of the antigen(s) recognized by TIL. If a common tumor antigen can be defined, it should enable us to effectively induce an anti-tumor immune response for therapy.

Cytotoxic T-cells play an important role in cellular immunity against tumors. It has been reported that CD8 positive anti-tumor T-cells infiltrate local lesions of human colorectal tumor tissue (10) and renal cell carcinoma (11). Furthermore, cytokines are key molecules that modulate the

function of T-cells. T helper type 1 cells (Th1), Th2, T cytotoxic 1 cells (Tc1), and Tc2 play immunoregulatory roles (12,13). Alterations of T cytotoxic type 1 (Tc1)/T cytotoxic type 2 (Tc2) subsets may cause host anti-tumor immune responses (14-16). Although cytokine expression patterns in TILs isolated from various tumor cell types have been reported, the changes of cytokine production in TILs are still somewhat controversial.

To elucidate the characteristics of T-cells infiltrating tumor tissues, we analyzed TCR variable region repertoires within tissue specimens from surgical lesions of patients with gastric or colorectal cancer. In addition, we analyzed T-cell clonalities by CDR3 size spectratyping with these tissues. We found similar TCR repertoires among multiple specimens from different sites of the same tumor, suggesting that the tumor-specific T-cells recognize common antigens in tumor lesions. Furthermore, we examined the expression levels of several cytokines such as IFN-γ and IL-4 by real-time quantitative polymerase chain reaction. The elevated levels of IFN-γ/IL-4 were observed in tumor lesions compared to PBMCs. The results suggest that polarization of TIL toward Th1/Tc1 subsets has an effect on the anti-tumor immune response.

Patients and methods

Patients and samples. Tissue specimens and peripheral blood mononuclear cells (PBMCs) were collected from 11 patients who underwent surgical operations at Tohoku University Hospital (Table I). The tissues were freshly collected from tumor specimens immediately after the surgical operations. Fresh specimens were collected from one or more different sites of tumor resected from the same patient. Each of the specimens was obtained from a location distant from the others by punch biopsy. The tissues were immediately frozen in liquid nitrogen for RNA extraction. Tissue samples in which lymphocyte infiltration was verified by histological testing were used for analyses. Normal tissue samples around tumor, in which few lymphocyte invasions were found, were used as a control. PBMCs were collected at the time of the operations. All samples used in the present study were collected after informed consent had been obtained.

TCR repertoire analysis. The methods for isolation of RNA from PBMCs and adaptor ligation-mediated polymerase chain reaction (PCR) were previously reported (17,18). Freshly isolated RNA was converted to double-stranded cDNA using Superscript cDNA synthesis kits (Invitrogen, CA) according to the manufacturer's instructions, except that a specific primer (BSL-18) was used. The P10EA/P20EA adaptors were ligated to the 5'-end of cDNA and this adaptor-ligated cDNA was cut with *NotI*. PCR was performed with T-cell receptor α-chain constant region (TCRAC)-specific or T-cell receptor β-chain constant region (TCRBC)-specific primers (CA1 or CB1) and P20EA. The second PCR was performed with CA2 or CB2 and P20EA. The third PCR was performed using both P20EA and 5'-biotinylated CA4 or CB4 primer for biotinylation of PCR products. TCRAV and TCRBV repertoires were analyzed by microplate hybridization assay (MHA) (17,18). In short, 10 pmol of amino-modified oligonucleotides specific for TCRAV and TCRBV segments

Table I. Patient characteristics.

Patient	Age	Sex	Diagnostic	Stage	Recurrent
1	64	M	Sigmoid colon	2	-
2	73	M	Gastric	1b	-
3	53	M	Sigmoid colon	4	-
4	68	M	Gastric	3a	+
5	65	M	Gastric		+
6	68	M	Transversum Colon	3a	-
7	73	M	Rectal	2	-
8	33	M	Rectal	3b	-
9	74	M	Rectal	2	-
10	70	F	Rectal	2	+
11	50	M	Rectal	3a	-

were immobilized onto carboxylate-modified 96-well microplates (C type, Sumitomo Bakelite, Tokyo, Japan) with water-soluble carbodiimide. Prehybridization and hybridization were performed in GMC buffer (0.5 M Na_2HPO_4, pH 7.0, 1 mM EDTA, 7% SDS and 1% BSA) at 47°C. Sixty microliters of denatured 5'-biotinylated PCR products mixed with an equivalent volume of 0.4 N NaOH/10 mM EDTA was added to 6 ml of GMC buffer. Hybridization solution, 100 μl, was used in each well of the microtiter plate containing immobilized oligonucleotide probes specific for the V segment. After hybridization, the wells were washed 6 times with washing buffer (2X SSC, 0.1% SDS) at room temperature and then with VA (0.4X SSC, 0.1% SDS) or VB (0.6X SSC, 0.1% SDS) stringency washing buffer for 10 min at 37°C. The blocking of non-specific binding was done with 200 μl of TB-TBS buffer [10 mM Tris-HCl, 0.5 M NaCl, pH 7.4, 0.5% Tween 20 and 0.5% blocking reagent (Roche Diagnostics, Germany)]. Next, 100 μl of a 1:1000-diluted, alkaline phosphatase-conjugated streptavidin (Invitrogen) in TB-TBS was added, and the sample was incubated at 37°C for 30 min. The plates were washed 6 times in T-TBS (10 mM Tris-HCl, 0.5 M NaCl, pH 7.4, 0.5% Tween 20). For color development, 100 μl of substrate solution (4 mg/ml p-nitro-phenylphosphate, Sigma, in 20% diethanolamine, pH 9.8) was added, and then absorbance was determined at 405 nm.

T-cell clonality analysis with CDR3 size spectratyping. PCR for CDR3 size spectratyping was performed for 30 cycles in a 20-μl volume under the same conditions as described above. PCR was performed with 1 μl of the second PCR product, 0.1 μM of 5'-Cy5 CA2/CB2, and 0.1 μM primer specific for each variable segment. The oligonucleotide probes for hybridization were used as primers specific for each variable segment. Five microliters of 1:20 or 1:50 diluted PCR product in dye solution (95% formamide, 10 mM EDTA and 0.1% blue dextrane) was analyzed in 6% denatured acrylamide gel with an ALFred sequence analyzer (Pharmacia Biotech, Uppsala, Sweden). The data obtained were transferred to Fragment Manager Software (Pharmacia Biotech). As a
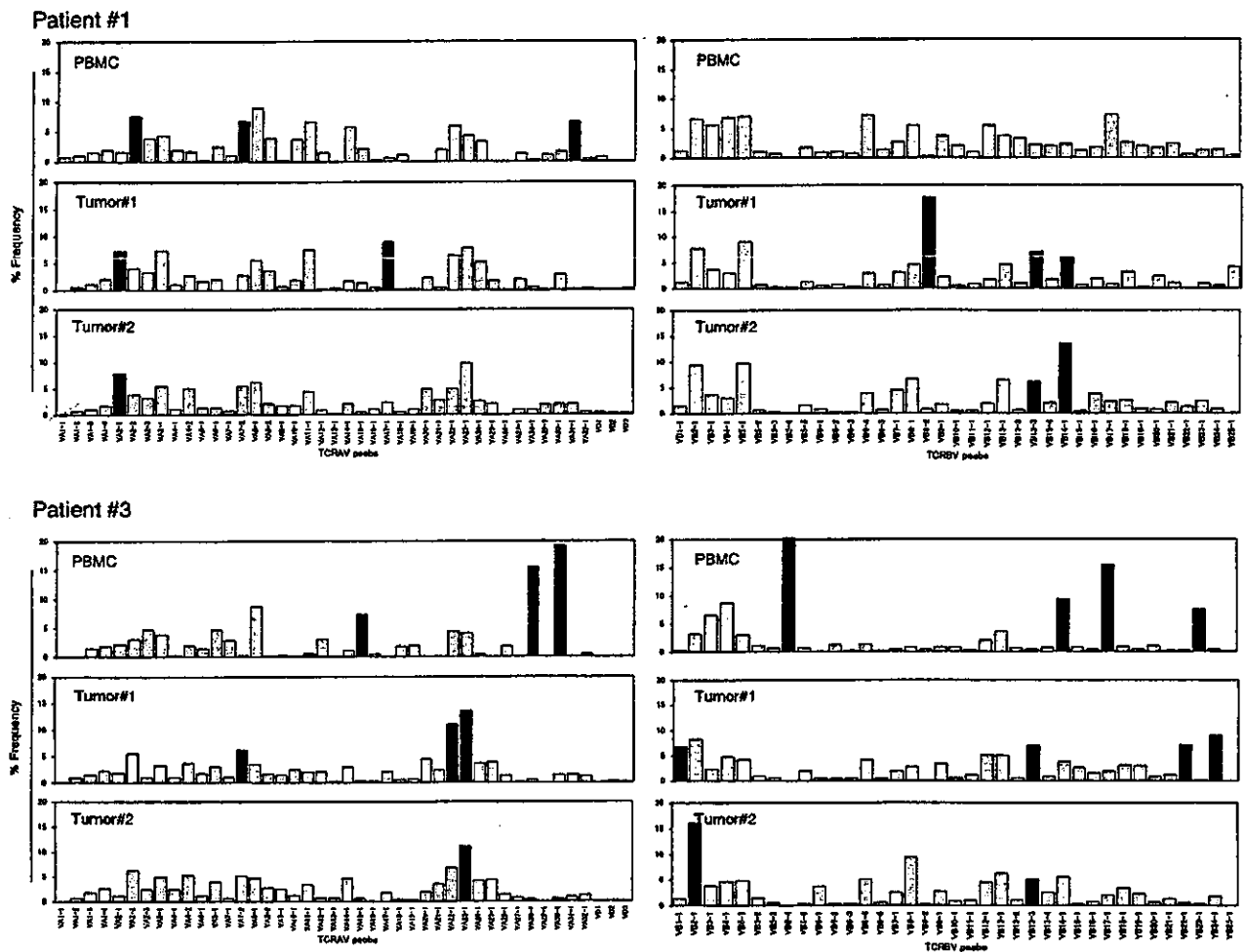
Patient #1

Patient #3

Figure 1. Representative results of T-cell receptor (TCR) variable region α-chain (TCRAV) and TCR β-chain (TCRBV) repertoires in patients with gastric or colorectal cancer. TCRAV (left) and TCRBV (right) repertoires were analyzed with a peripheral blood mononuclear lymphocyte (PBMC) and two samples from different sites of the same tumor. Percent frequencies of expression levels in each segment are shown. The segments, in which a high level of expression above the control levels was found, are shown by closed bars.

control, PBMCs from 10 healthy donors were also analyzed for the peak patterns, revealing multiple peaks as Gaussian patterns with 3-nucleotide intervals in each V segment.

Quantification of cytokine mRNA. The expression levels of mRNA of interleukin-2 (IL-2), interferon-γ (IFN-γ), inter-leukin-4 (IL-4), interleukin-5 (IL-5), and tumor necrosis factor-α (TNF-α) were examined for PBMCs, normal tissues and tumor lesions of patients with real-time quantitative polymerase chain reaction (PCR) using GeneAmp 5700 Sequence Detector (Applied Biosystems, CA). Freshly isolated RNA was converted to cDNA using Superscript™ reverse transcriptase II (Invitrogen, CA). Next, one-tenth of the cDNA was amplified with qPCR Mastermix for Sybr™ Green I (Eurogentec, Belgium) according to the manufacturer's instructions. Primer pairs specific for each cytokine gene were used (19). The C_T, or threshold cycles, values were obtained with 10-fold dilution of PCR products ranging from 20 to 0.0002 amol/ml within the exponential phase of the PCR. For standard curves, the C_T values were plotted against the known amount of PCR products. Glyceraldehyde-3-

phosphate dehydrogenase (GAPDH) gene was used for the internal control. The results were expressed as the ratio of the amount of the respective cytokine-specific cDNA to the amount of GAPDH-specific cDNA.

Determination of nucleotide sequence of CDR3 regions. PCR was performed with a forward primer specific for the variable region (VA7-2 or VB13-2) and a reverse primer specific for the constant region (CA4 or CB4) under conditions described above. Primer used in this study was as follows: VA7-2-: TTCCTTAGTCGGTCTAAAGGG, VB13-2: GAATTTCCT GCTGGGGTTGG, CA4: ATAGGCAGACAGACTTGTCA CTG, CB4: ACACCAGTGTGGCCTTTTGGGTG. After the PCR products were eluted from agarose gel, the PCR products were cloned into pCR2.1-TOPO vector with TOPO TA Cloning kit (Invitrogen, CA). DH5α-T1* competent cells were transformed with the recombinant plasmid DNA. Sequence reaction were performed with BigDye® Terminator v3.0 Cycle Sequencing Kit (Applied Biosystems, CA) and analyzed by ABI PRISM 3100 genetic analyzer (Applied Biosystems).

Table II. TCRAV and TCRBV segments with a high level of expression.[a]

Patient	Source	TCRAV	TCRBV
1	PBMC	2-2, 7-2, 31-1	-
	Tumor no. 1	2-1, 17-1	8-2, 13-3, 14-1
	Tumor no. 2	2-1	13-3, 14-1
2	PBMC	2-1, 24-1, 25-1	4-1, 16-1
	Tumor no. 1	-	8-1
	Tumor no. 2	25-1	-
	Tumor no. 3	21-1	-
3	PBMC	15-1, 28-1, 30-1	5-4, 14-1, 17-1, 23-1
	Tumor no. 1	7-2, 22-1, 23-1	1-1, 13-3, 22-1, 24-1
	Tumor no. 2	23-1	2-1, 13-3
4	PBMC	1-4, 10-1, 12-1, 13-1	6-4, 10-1
	Normal tissue	12-1	8-1
	Tumor no. 1	12-1	-
	Tumor no. 2	12-1, 21-1	7-1, 13-3
	Tumor no. 3	-	-
5	PBMC	2-1, 6-1, 23-1	13-4
	Tumor no. 1	13-1, 23-1	6-5
	Tumor no. 2	23-1	6-5
	Tumor no. 3	13-1, 23-1	6-5
6	PBMC	17-1, 22-1, 30-1	24-1
	Tumor no. 1	21-1, 29-1	8-1
7	PBMC	2-3, 24-1	8-2
	Normal tissue	21-1	6-5, 8-1, 12-1
8	PBMC	-	15-1
	Tumor no. 1	20-1	8-1, 13-3
9	PBMC	23-1	9-1
	Tumor no. 1	24-1	2-1, 13-1
10	PBMC	-	5-1
	Tumor no. 1	4-2, 7-2	7-1, 13-2
	Tumor no. 2	17-1, 21-1, 30-1	6-5, 13-2
11	PBMC	21-1	5-1
	Tumor no. 1	3-1, 4-2, 20-1, 21-1	-
	Tumor no. 2	3-1, 4-2, 23-1	13-3
	Tumor no. 3	3-1, 16-1, 20-1, 21-1	6-5

[a]Significant increase in frequency was defined as follows: the percentage was greater than the mean percentage + 3 standard deviations of PBLs from 20 healthy controls, and the absolute percentage was >5%.

Statistical analysis. Data were statistically analyzed by the Wilcoxon rank-sum test.

Results

TCRAV and TCRBV repertoires in tumor lesions and PBMCs. TCRAV and TCRBV repertoires were analyzed by microplate hybridization assay. The expression levels of mRNA were quantitatively analyzed with 43 oligonucleotide probes specific for α-chain variable segments and 37 probes specific for ß-chain variable segments. Almost all TCRAV and TCRBV segments defined in WHO nomenclature as functional segments can be detected with these probes.

TCR repertoires were analyzed for 11 tumors (total 21 samples), 2 normal tissues, and 11 peripheral blood mononuclear cells (PBMCs) from 11 patients (Table I). The representative results of TCR repertoire analysis are shown in Fig. 1. We defined the increase as significant, when: i) the
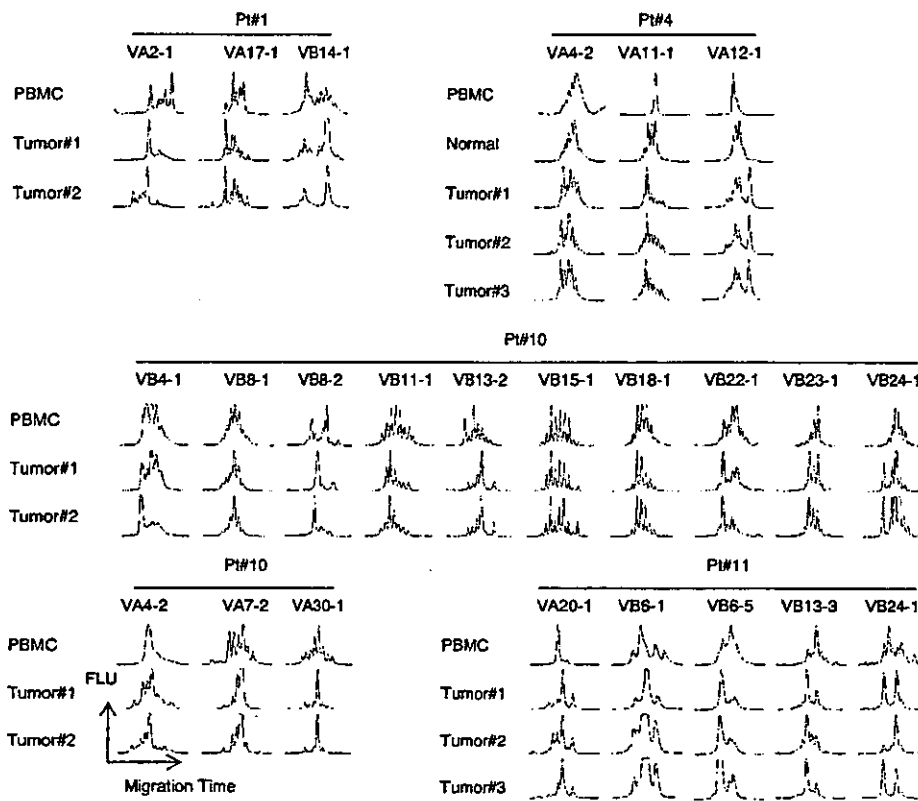
Figure 2. Similarities of CDR3 size spectratyping patterns among multiple samples from different sites of the same tumor. CDR3 spectratyping was performed with PBMCs and tumor tissues obtained from a large number of tumor patients. Representative peak patterns, which had identical peaks in size among multiple tumor samples from the same patient, are shown. X-axis, migration time; Y-axis, fluorescent intensity. Each peak was distributed along the X-axis according to their migration time.

percentage was greater than the mean percentage + 3 standard deviations of PBMCs from 20 healthy controls, and ii) the absolute percentage was >5%. The expression level was defined as uncharged unless the numbers fulfilled these two criteria. There were significant increases in the usage of TCRAV and TCRBV repertoires in tumor lesions, normal tissues, and PBMCs.

In PBMCs, the mean number of variable segments, of which the frequency was significantly increased above the control levels, was 2.1±1.4 (mean ± SD) per patient for TCRAV and 1.4±1.0 per patient for TCRBV. On the other hand, the mean number was 1.8±1.1 per patient for TCRAV and 1.3±1.1 per patient for TCRBV in tumor lesions. There is no difference in the mean numbers of variable segments between tumor lesions and PBMCs. The results are summarized in Table II. Restricted usage of TCRAV and TCRBV repertoires was not observed in PBMCs from tumor patients. In contrast, significant increases above the control were frequently detected in limited AV and BV segments such as VA21-1 [5 per 11 patients (45%)] and VB13-3 [5/11 (45%)] in tumor lesions.

In AV25-1 of patient 2, VA12-1 of patient 4, VA23-1 of patient 5 and VA21-1 of patient 11, significant increases in the frequency were detected in both PBMC and tumor lesions. In contrast, significant increases were observed within PBMC alone in most variable segments other than these segments. The result indicates a difference in the TCRAV and TCRBV repertoires between PBMCs and tumor

lesions in individual patients. Significant increases in the frequency were observed in common variable segments among two or more samples from different sites of the same tumor. For example, VA2-1, VB13-3 and VB14-1 of patient 1, VA23-1 and VB13-3 of patient 3, VA13-1 and VB6-5 of patient 5, VB13-2 of patient 10, VA3-1, VA4-2 and VA20-1 of patient 11, VA3-1 of patient 11 and VB6-5 of patient 5 were significantly higher in three tumor samples, but not in PBMC. The results show that similar TCRAV and TCRBV repertoires were used for T-cell populations among samples from different sites of the same tumor.

T-cell clonality in tumor. We tried to demonstrate whether oligoclonal or monoclonal T lymphocytes exist in local tumor lesions. First. we examined T-cell clonality with CDR3 size spectratyping in a large number of BV segments, in which the frequency was significantly higher above the controls. The normal pattern displays multiple peaks with a Gaussian pattern with 3-nucleotide intervals. When a clonal T-cell expands in a variety of T-cell populations, a single higher peak appears within multiple low peaks. The clonal peak, which means clonal expansion of T-cells, was detected in a variety of BV segments with PBMCs and tumor lesions. Similar patterns of CDR3 size spectratyping were found among two or more samples from different sites of the same tumor. Interestingly, identical peaks of the same length were detected among multiple samples from the same tumor (Fig. 2). The results showed that a limited number of T-cells infiltrate
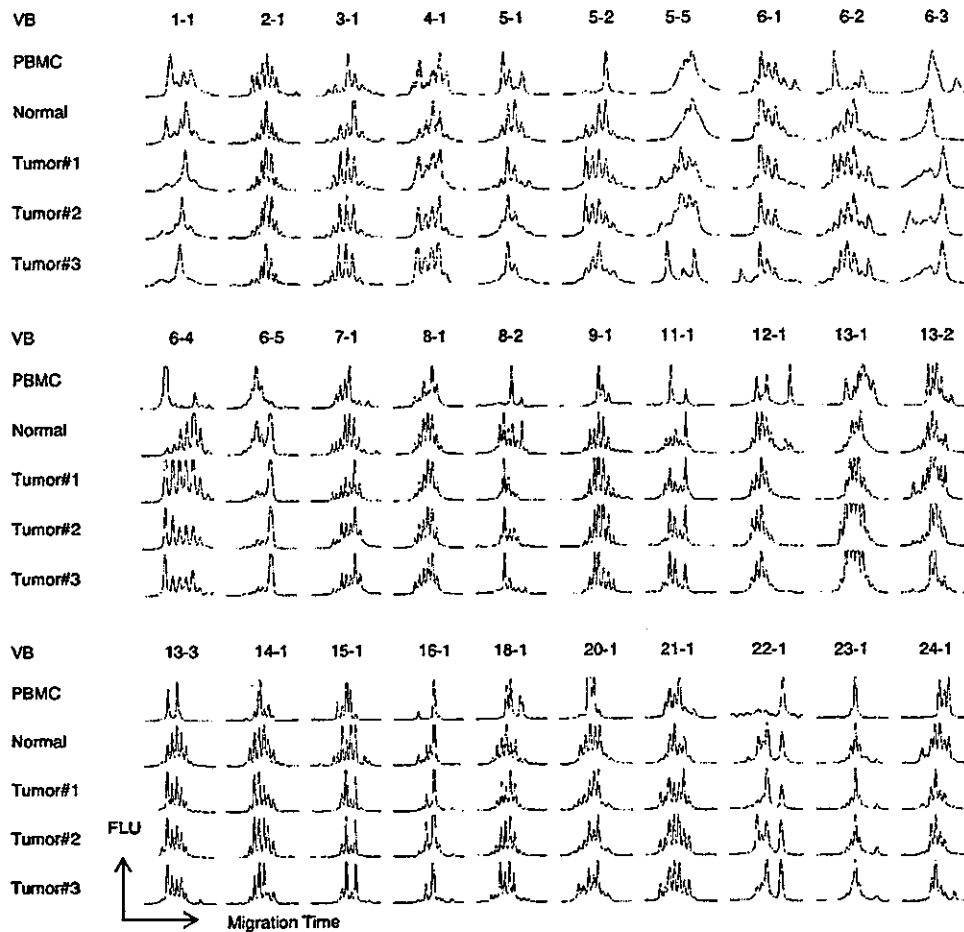
Figure 3. CDR3 size spectratyping profiles of PBMC, tumor lesion, and normal tissue. CDR3 spectratyping was performed with a peripheral blood mononuclear cell (PBMC), a normal tissue (normal), and three tumor lesions (tumor) obtained from patient 4. Similar spectratyping patterns were observed among three tumor lesions in a majority of the VB segments analyzed. In contrast, the spectratyping patterns for tumor lesions were different from that for PBMC and normal tissue.

into tumor tissues. We also performed the spectratyping with normal tissue around a tumor in which few lymphocyte infiltrations were found (Fig. 3). The result showed that the spectratyping patterns obtained with the normal tissue were different from that with tumor lesions from the same patient. This indicated that the appearance of clonal or oligoclonal T-cells was not due to non-specific activation or contamination of peripheral lymphocytes. Next, to examine whether clonal peaks with similar size are due to clonal expansion of identical T-cells, we determined nucleotide sequences of CDR3 region of cDNA clones obtained from multiple tumor lesions and PBMC from the same patient (Table III). The result showed that cDNA clones with identical nucleotide sequence were obtained from two tumor lesions, but not from PBMC. Furthermore, these cDNA clones existed frequently in tumor lesions, which was consistent with the result from CDR3 size spectratyping. There was no common motif or conserved amino acid sequences of CDR3 regions among these cDNA clones.

Cytokine expression in local tumor lesions and PBMCs. We examined the expression levels of mRNA of interleukin-2 (IL-2), interleukin-4 (IL-4), interleukin-5 (IL-5), interferon-γ

(IFN-γ), and tumor necrosis factor-α (TNF-α) in PBMCs (n=11) and tumor lesions (n=21) by real-time quantitative polymerase chain reaction (Fig. 4). There was no difference of the expression levels of IL-5 and IFN-γ between tumor lesions and PBMCs. In contrast, the expression levels of IL-2, IL-4, and TNF-α were lower in tumor lesions than in PBMCs (p<0.005). Especially the expression level of IL-4 was considerably lower in tumor lesions compared with PBMCs.

The tumor specimens are thought to contain a large amount of non-lymphocyte cells derived from cancers. Therefore, a difference of the number of cytokine-producing cells such as T-cells and monocytes may have existed between tumor lesions and PBMCs. We thus compared the balance of T helper 1 (Th1) or T cytotoxic 1 (Tc1) to T helper 2 (Th2) or T cytotoxic 2 (Tc2), which was shown by the ratio of the levels of TNF-γ to that of IL-4, between tumor lesions and PBMCs. The ratio of IFN-γ to IL-4 was significantly higher for tumor lesions than PBMCs (p<0.05) (Fig. 5).

Discussion

Tumor-infiltrating lymphocytes (TILs) respond against tumor antigens at local sites (20). To elucidate the characteristics

Table III. Alignment of amino acid sequences of CDR3 regions from cDNA clones.

Source	Frequency	AV/BV Segment	AV/BV sequence	N/N-D-N	AJ/BJ sequence	AJ/BJ Segment
PBMC	1/3	BV13S2	YFCASSY	GTPFGDTPFG	DTQYFGPGTRLTVL	BJ2S3
	1/3	BV13S2	YFCASSY	KH	EQFFGPGTRLTVL	BJ2S1
	1/3	BV13S2	YFCASSY	SPGQGA	GYTFGSGTRLTVV	BJ1S1
Tumor no. 1	3/5	BV13S2	YFCASSY	TTSG	SYEQYFGPGTRLTVT	BJ2S7
	1/5	BV13S2	YFCASS	SVSGQLQ	AFFGQGTRLTVV	BJ1S1
	1/5	BV13S2	YFCASSY	PFGTFP	NTGELFFGEGSRLTVL	BJ2S2
Tumor no. 2	2/4	BV13S2	YFCASSY	TTSG	SYEQYFGPGTRLTVT	BJ2S7
	1/4	BV13S2	YFCAS	TDTGTTYR	AFFGQGTRLTVV	BJ1S1
	1/4	BV13S2	YFCASSY	QSLGQGAF	TEAFFGQGTRLTVV	BJ1S1
PBMC	1/5	AV7S2	YLCAV	ITDS	WGKLQFGAGTQVVVTP	AJ24
	1/5	AV7S2	YLCAV	THR	NYGQNFVFGPGTRLSVLP	AJ26
	1/5	AV7S2	YLCAV	QPFY	GGYQKVTFGTGTKLQVIP	AJ13
	1/5	AV7S2	YLCA	ATLLG	AGNNRKLIWGLGTSLAVNP	AJ38
	1/5	AV7S2	YLCAVR	PI	SDGQKLLFARGTMLKVDL	AJ16
Tumor no. 1	4/5	AV7S2	YLCAVR	DMA	NAGKSTFGDGTTLTVKP	AJ27
	1/5	AV7S2	YLCAV	V	DSNYQLIWGAGTKLIIKP	AJ33
Tumor no. 2	3/4	AV7S2	YLCAVR	DMA	NAGKSTFGDGTTLTVKP	AJ27
	1/4	AV7S2	YLCAV	THR	NYGQNFVFGPGTRLSVLP	AJ26

All samples were obtained from patient no. 10. TCRAV and BV gene segments were described according to the nomenclature reported by Arden *et al* (26) and Wei *et al* (27). TCRAJ and BJ gene segments were also described according to the nomenclature reported by Koop *et al* (28) and Toyonaga *et al* (29).
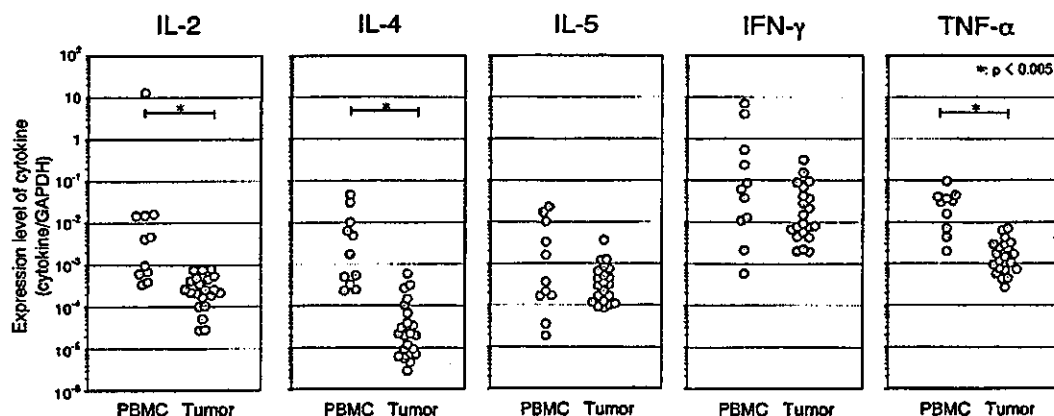

Figure 4. Comparison of the expression levels of several cytokines between tumor lesions (n=21) and PBMCs (n=11). The expression levels of mRNA of interleukin-2 (IL-2), interleukin-4 (IL-4), interleukin-5 (IL-5), interferon-γ (IFN-γ), and tumor necrosis factor-α (TNF-α) were measured by real-time quantitative polymerase chain reaction as described in Materials and methods. Each open dot indicates a single sample. Glyceraldehyde-3-phosphate dehydrogenase (GAPDH) gene was used for the internal control. The levels of mRNA expressed by the ratio of the amount of the respective cytokine-specific cDNA to the amount of GAPDH-specific cDNA were compared between PBMC and tumor lesions. The expression levels of IL-2, IL-4, and TNF-α were lower in tumor lesions than in PBMCs (p<0.005).

of TILs in local microenvironments, we analyzed T-cell receptor (TCR) repertoires at the levels of mRNA with tissue samples and PBMCs. It is possible that *in vitro* culture in the presence of IL-2 causes skewing of TCR variable region repertoires (21). We therefore directly analyzed tissue samples freshly removed from tumor specimens of surgical patients. This enabled us to accurately analyze the TCR repertoire with a small amount of tissues containing a limited number
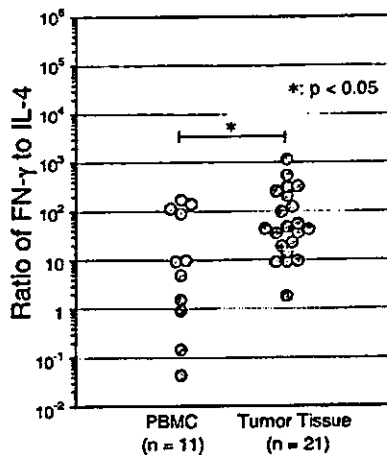
Figure 5. Predominant production of T helper 1/T cytotoxic 1 type cytokine in tumor lesions. Ratio of the expression levels of IFN-γ to that of IL-4 were compared between tumor lesions (n=21) and PBMCs (n=11). Each open dot indicates a single sample. The ratio was significantly higher in tumor lesions than in PBMCs (p<0.05).

of TILs. Clonal expansion of T-cells in renal cell carcinoma has been already reported (8). In the report, many sets of variable region-specific primer were used for analysis of TCR repertoire. However, different amplification efficiencies among individual primers or cross-reactivity between sub-families hampered the accurate estimation of the frequency of individual families. An adaptor ligation-mediated PCR used in this study is more efficient and less skewing through PCR cycles than other PCR-based methods.

The frequencies of one or more variable segments were significantly increased in most of the tissue samples analyzed. There was, however, no difference of the mean number of variable segments, of which the frequency increased significantly, between tumor lesions and PBMCs. This indicates that the extent of skewing of TCR repertoires was not different between tumor lesions and PBMCs. This does not necessarily mean that the immunological alterations did not occur in local sites around the tumor. We observed that several variable segments were frequently used in tumor lesions, but not in PBMCs. This finding suggested that TILs have a limited TCR repertoire and may recognize a common tumor-specific antigen. The possibility exist that non-specific inflammation of T-cells at local sites or the homing of T-cells with a limited TCR repertoire to an inflamed site may induce the skewing of TCR repertoires. However, we observed a similarity of TCR repertoire among multiple samples from different sites of the same tumor. Such similarity was not detected between tumor lesions and normal tissues or between tumor lesions and PBMCs. This suggests that a limited number of antigen-specific TILs infiltrate into multiple local sites around a tumor. It is known that the TCR repertoire becomes skewed with aging as a result of clonal expansion (22,23). Because the tumor patients used in this study were mostly elderly. skewed TCR repertoires could be expected even in PBMCs.

We analyzed T-cell clonality with CDR3 size spectratyping. The clonality analysis coupled with quantitative analysis of

the TCR repertoire could provide important information about TILs. When tissue samples containing a small number of T-cells are used for the clonality analysis, the clonality might be increased through PCR cycles. However, the increase of clonality accompanied by an elevated frequency of expression offers firm evidence for a large population of oligoclonal or clonal T-cells existing within local tumor lesions. We found the increase of T-cell clonality in a majority of TCR variable segments, with higher frequencies than the controls. We also detected similar peak patterns of CDR3 spectratyping among multiple samples from different sites of the same tumor. The cDNA clones with identical nucleotide sequence of CDR3 region were obtained from two tumor samples of the same patient. These results suggest that a limited number of TILs proliferate within local sites in response to tumor antigen. The elevated level of clonality was also found in PBMCs of tumor patients. However, we were able to find a difference of spectratyping peak patterns between tumor lesions and PBMCs. Sequence analysis indicated that clonal T-cells existing frequently in tumor lesions were not observed in PBMC. This excludes the possibilities of non-specific expansion of T-cells or the homing of T-cells from peripheral blood lymphocytes to inflammatory sites. Instead, this suggests that a limited number of TILs locally expanded in response to tumor antigens.

T-cells are functionally characterized by the pattern of cytokine productions, i.e., T helper 1 (Th1)/T cytotoxic 1 (Tc1) and T helper 2 (Th2)/T cytotoxic 2 (Tc2). In addition, local production of cytokines probably impacts on the function of T-cells infiltrating into tumor tissues. Thus, we quantitatively measured the amounts of cytokine mRNA in tumor lesions and PBMCs. Similar levels of IL-5 and IFN-γ were observed between PBMCs and tumor lesions, whereas low levels of expression of IL-2, IL-4 and TNF-α were found in tumor lesions. It has been reported that IL-2, IFN-γ and TNF-β were not expressed at higher levels in the TIL of lung carcinoma patients (24). Our results did not indicate high level expression of IFN-γ or TNF-α, which is thought to be Th1-type cytokine, in tumor lesions. Instead, the data showed an apparent decrease in IL-4 production in tumor lesions. Although freshly isolated tissue specimen was suitable for direct estimation of the cytokine profile in a local microenvironment, the tissues contained a large amount of non-lymphocyte cells derived from the tumor. Thus, it may be difficult to directly compare the expression levels of cytokine mRNA between tumor lesions and PBMCs. The balance of Th1/Tc1-type cytokine to Th2/Tc2-type cytokine is meaningful for understanding the immunological status at local sites. The ratio of IFN-γ to IL-4 was significantly increased in tumor lesions compared with PBMCs. This suggests that Th1/Tc1-type cells may selectively infiltrate into the local tissues. However, another possibility that IL-4-producing Th2 cells accumulated in PBMC of tumor patients can be proposed. To clarify these possibilities, the levels of IFN-γ and IL-4 mRNA might need to be measured in PBMC from age-matched healthy donors. It has been reported that TILs were characterized by a type 1 (Th1/Tc-1-like) pattern of cytokine expression in human colorectal carcinoma (25). No or only very small amounts of IL-4 transcripts have been detected in TIL. Our results are

consistent with this report. Th1 and Tc1 promote cellular immunity through the production of type 1 cytokines, such as IL-2 and IFN-γ. Alteration of the cytokine pattern may promote TILs to strengthen the anti-tumor response although TILs cannot control tumor growth.

In conclusion, similar usage of the TCR variable region repertoire and a similar peak pattern of CDR3 spectratyping were frequently observed among different tissue samples from the same patients with gastric and colorectal cancers. These results suggest that TILs proliferate locally in response to tumor antigens. Predominant Th1/Tc1-type cytokine to Th2/Tc2 (IFN-γ/IL-4) was apparently found in tumor lesions. These results show that T helper type 1 (Th1) and T cytotoxic type 1 (Tc1) may exert immunoregulatory effects on anti-tumor immune responses.

References

1. Boon T, Cerottini JC, van den Eynde B, van der Bruggen P and van Pel A: Tumor antigens recognized by T lymphocytes. Annu Rev Immunol 12: 337-365, 1994.
2. Vose BM and Moore M: Human tumor-infiltrating lymphocytes: a marker of host response. Semin Hematol 22: 27-40, 1985.
3. Coulie PG, Brichard V, van Pel A, et al: A new gene coding for a differentiation antigen recognized by autologous cytolytic T lymphocytes on HLA-A2 melanomas. J Exp Med 180: 35-42, 1994.
4. Kawakami Y, Eliyahu S, Delgado CH, et al: Identification of a human melanoma antigen recognized by tumor-infiltrating lymphocytes associated with in vivo tumor rejection. Proc Natl Acad Sci USA 91: 6458-6462, 1994.
5. Kawakami Y, Eliyahu S, Sakaguchi K, et al: Identification of the immunodominant peptides of the MART-1 human melanoma antigen recognized by the majority of HLA-A2-restricted tumor infiltrating lymphocytes. J Exp Med 180: 347-352, 1994.
6. Boon T, Coulie PG and van den Eynde B: Tumor antigens recognized by T-cells. Immunol Today 18: 267-268, 1997.
7. Hogan KT, Eisinger DP, Cupp SB III, et al: The peptide recognized by HLA-A68.2-restricted, squamous cell carcinoma of the lung-specific cytotoxic T lymphocytes is derived from a mutated elongation factor 2 gene. Cancer Res 58: 5144-5150, 1998.
8. Gaudin C, Dietrich PY, Robache S, et al: In vivo local expansion of clonal T-Cell subpopulations in renal cell carcinoma. Cancer Res 55: 685-690, 1995.
9. Davis MM and Bjorkman PJ: T-cell antigen receptor genes and T-cell recognition. Nature 334: 395-402, 1988.
10. Naito Y, Saito K, Shiiba K, Ohuchi A, Saigenji K, Nagura H and Ohtani H: CD8+ T-cells infiltrated within cancer cell nests as a prognostic factor in human colorectal cancer. Cancer Res 58: 3491-3494, 1998.
11. Nakano O, Sato M, Naito Y, et al: Proliferative activity of intratumoral CD8(+) T-lymphocytes as a prognostic factor in human renal cell carcinoma: clinicopathologic demonstration of antitumor immunity. Cancer Res 61: 5132-5136, 2001.
12. Abbas AK, Murphy KM and Sher A: Functional diversity of helper T lymphocytes. Nature 383: 787-793, 1996.
13. Mosmann TR, Li L and Sad S: Functions of CD8 T-cell subsets secreting different cytokine patterns. Semin Immunol 9: 87-92, 1997.
14. Sad S, Marcotte R and Mosmann TR: Cytokine-induced differentiation of precursor mouse CD8+ T-cells into cytotoxic CD8+ T-Cells secreting Th1 or Th2 cytokines. Immunity 2: 271-279, 1995.
15. Cerwenka A, Carter LL, Reome JB, Swain SL and Dutton RW: In vivo persistence of CD8 polarized T-cell subsets producing type 1 or type 2 cytokines. J Immunol 161: 97-105, 1998.
16. Li L, Sad S, Kagi D and Mosmann TR: CD8Tc1 and Tc2 cells secrete distinct cytokine patterns in vitro and in vivo but induce similar inflammatory reactions. J Immunol 158: 4152-4161, 1997.
17. Matsutani T, Yoshioka T, Tsuruta Y, Iwagami S and Suzuki R: Analysis of TCRAV and TCRBV repertoires in healthy individuals by microplate hybridization assay. Hum Immunol 56: 57-69, 1997.
18. Matsutani T, Yoshioka T, Tsuruta Y, et al: Restricted usage of T-cell receptor alpha-chain variable region (TCRAV) and T-cell receptor beta-chain variable region (TCRBV) repertoires after human allogeneic haematopoietic transplantation. Br J Haematol 109: 759-769, 2000.
19. Mempel M, Musette P, Flageul B, et al: T-cell receptor repertoire and cytokine pattern in granuloma annulare: defining a particular type of cutaneous granulomatous inflammation. J Invest Dermatol 118: 957-966, 2002.
20. Wang RF and Rosenberg SA: Human tumor antigens for cancer vaccine development. Immunol Rev 170: 85-100, 1999.
21. Dietrich PY, Walker PR, Schnuriger V, et al: TCR analysis reveals significant repertoire selection during in vitro lymphocyte culture. Int Immunol 9: 1073-1083, 1997.
22. Schwab R, Szabo P, Manavalan JS, et al: Expanded CD4+ and CD8+ T-cell clones in elderly humans. J Immunol 158: 4493-4499, 1997.
23. Wack A, Cossarizza A, Heltai S, et al: Age-related modifications of the human alphabeta T-Cell repertoire due to different clonal expansions in the CD4+ and CD8+ subsets. Int Immunol 10: 1281-1288, 1998.
24. Roussel E, Gingras MC, Grimm EA and Roth JA: High expression of adhesion molecules/activation markers with little interleukin-2, interferon gamma, and tumor necrosis factor beta gene activation in fresh tumor-infiltrating lymphocytes from lung adenocarcinoma. Cancer Immunol Immunother 41: 1-9, 1995.
25. Csiszar A, Szentes T, Haraszti B, Zou W, Emilie D, Petranyi G and Pocsik E: Characterization of cytokine mRNA expression in tumor-infiltrating mononuclear cells and tumor cells freshly isolated from human colorectal carcinomas. Eur Cytokine Netw 12: 87-96, 2001.
26. Arden B, Clark SP, Kabelitz D and Mak TW: Human T-cell receptor variable gene segment families. Immunogenetics 42: 455-500, 1995.
27. Wei S, Charmley P, Robinson MA and Concannon P: The extent of the human germline T-cell receptor V beta gene segment repertoire. Immunogenetics 40: 27-36, 1994.
28. Koop BF, Rowen L, Wang K, et al: The human T-cell receptor TCRAC/TCRDC (C alpha/C delta) region: organization, sequence, and evolution of 97.6 kb of DNA. Genomics 19: 478-493, 1994.
29. Toyonaga B, Yoshikai Y, Vadasz V, Chin B and Mak TW: Organization and sequences of the diversity, joining, and constant region genes of the human T-cell receptor beta chain. Proc Natl Acad Sci USA 82: 8624-8628, 1985.

II. 骨代謝調節系

破骨細胞の機能・骨吸収メカニズム 骨吸収促進因子

破骨細胞分化因子RANKL

Possible role of RANKL in bone resorption

宇田川信之[1] 中村美どり[2] 髙橋直之[3]

Key words：RANKL，OPG，破骨細胞，骨芽細胞，骨代謝共役因子

1. RANKL(receptor activator of NF-κB ligand)の発見

1997年，3つの異なる研究グループ(雪印乳業，アムジェン，スミスクラインビーチャム)によって破骨細胞形成を抑制する新規因子のcDNAクローニングが成功し，ほぼ同時期に報告された[1]．この同一分子(骨を防御する因子として命名されたosteoprotegerin(OPG)という統一名称を使用することが米国骨代謝学会で決議された)は，TNF受容体ファミリーでありながら膜貫通領域が存在しない分泌性の蛋白質であった[1]．

更に，雪印乳業のグループは，OPGが結合するリガンドとしてTNFファミリーに属する膜結合蛋白質のcDNAのクローニングに成功した[2]．この分子こそ，骨芽細胞の細胞膜表面上に発現誘導される破骨細胞分化因子(ODF)そのものであった．ODFの細胞内領域と膜貫通領域を欠如した可溶性ODFを遺伝子工学的に作製し，破骨細胞分化誘導活性をマウスあるいはヒトの血液細胞の培養系を用いて調べたところ，骨芽細胞の非存在下でも可溶性ODFとマクロファージコロニー刺激因子(M-CSF)の添加によって破骨細胞が多数形成された．これらの破骨細胞形成促進活性はOPGの添加によって完全に阻害された[2]．

ODFの真の受容体は，既に報告されていたRANK(receptor activator of NF-κB)と呼ばれるTNF受容体ファミリーに属する膜結合蛋白質であることが種々の実験により証明された．したがって現在，ODFはRANKリガンド(RANKL)という名称で統一されている[1](図1)．

一方，OPGはRANKLのおとり受容体(decoy receptor)としてRANKLの真の受容体であるRANKと競合し，RANKよりもはるかに高い親和性でRANKLに結合することにより，RANKLの活性を抑制することが明らかとなった[1](図1)．RANKL遺伝子欠損マウスは破骨細胞の欠如により大理石骨病を呈することより，RANKLの破骨細胞分化における重要性が証明されている[3]．

2. 活性化Tリンパ球に発現するRANKLは破骨細胞の分化を直接促進する

RANKLは破骨細胞の分化のみならずリンパ節の発生およびリンパ球の分化にも重要な役割を果たしていることが，RANKL遺伝子欠損マウスの所見から明らかとなり，免疫系におけるRANKLの重要性が注目されている[3]．

最近，関節リウマチ(RA)患者およびリウマチモデル動物の関節滑膜組織におけるRANKL

[1]Nobuyuki Udagawa: Department of Biochemistry, Matsumoto Dental University 松本歯科大学生化学 [2]Midori Nakamura: Department of Pediatric Dentistry 同小児歯科学 [3]Naoyuki Takahashi: Division of Hard Tissue Research, Institute for Oral Science 同総合歯科医学研究所硬組織疾患制御再建学
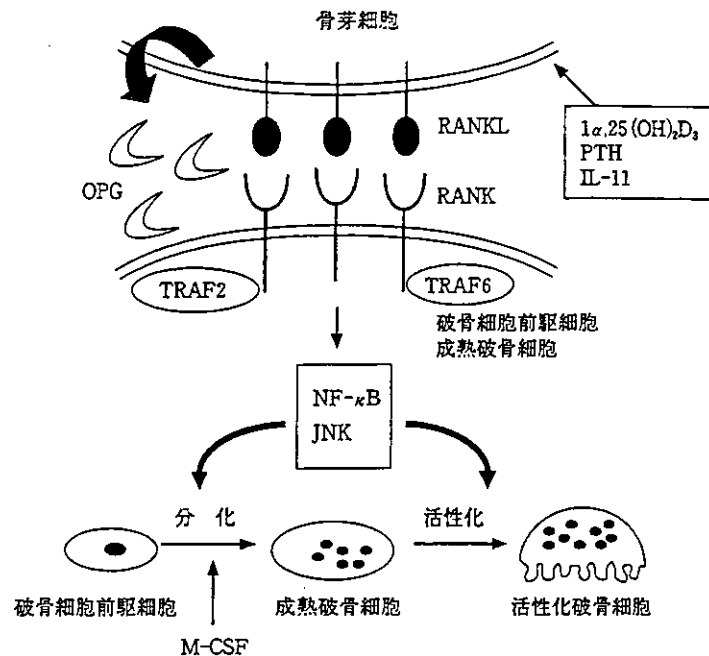
図1　破骨細胞形成の分子機構

の発現を解析した実験成績が相次いで報告された. 著者らも, *in situ* hybridization 法を用いて観察したところ, RA患者の関節滑膜組織において多数増殖が認められる線維芽細胞およびCD3陽性の活性化Tリンパ球にRANKLのmRNAおよび蛋白の発現を認めた[4]. また, RA患者の関節液中の可溶性RANKL濃度をELISA法によって測定した結果, RA患者の関節液中には, 変形性関節症, 外傷, 痛風患者と比較して, 可溶性RANKLが高濃度に含まれていることが明らかとなった. 一方, RA患者のOPG濃度は低値を示しており, 変形性関節症または痛風患者と比較すると, RA患者の関節液における可溶性RANKLとOPG濃度の比(RANKL/OPG)は有意に高値を示した. その結果, RANKL/OPGの上昇が, RAにおける骨破壊を惹起している可能性が示された[4]. 実際, 活性化されたTリンパ球がRANKLを発現し, 直接破骨細胞の分化を促進する実験結果も得られている(図2).

以上の *in vitro* の実験結果を支持する *in vivo* の実験結果として, マウスの関節炎モデルにお

ける骨破壊はRANKL遺伝子欠損マウスでは認められないとする実験成績が報告された[5]. また, アムジェンのグループは, Tリンパ球が恒常的に活性化されている ctla4 遺伝子欠損マウスは骨吸収の亢進が認められ典型的な骨粗鬆症の症状を示すこと, リウマチモデルであるアジュバント誘発関節炎ラットに対するOPGの投与は骨密度の回復作用を示すことを報告した[6]. 更に, 限局性若年性歯周炎の原因菌である *Actinobacillus actinomycetemcomitans* によって発症させた歯周炎モデルマウスにおける歯槽骨の吸収には活性化Tリンパ球(CD4$^+$ T cell)が直接関与しており, これらの骨吸収の亢進はOPGの投与によって抑制されるとする興味深い実験結果も報告されている[7].

また, RAの滑膜組織に存在するTリンパ球やマクロファージが産生するIL-6, 可溶性IL-6受容体(sIL-6R), IL-17, TNFα, IL-1α などは骨芽細胞に作用し, RANKLの発現を促すことにより破骨細胞の形成を促進するとする実験結果や, TNFやIL-1がRANKLを介さずに直接破骨細胞の分化や機能を制御するとする報告も
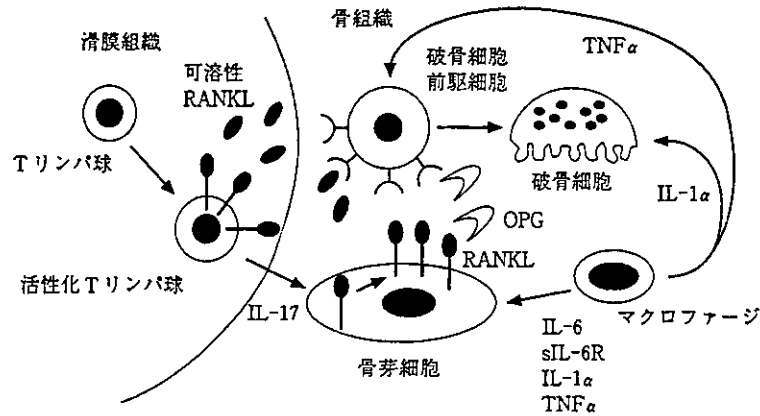
図2 活性化Tリンパ球の破骨細胞分化への関与

あり，RA病変における骨破壊には複数の機構が関与していると考えられる[7]（図2）.

東京大学医学部整形外科の田中らのグループは，自己RANKLに対する液性免疫誘導によりマウスの関節炎モデルにおける関節破壊を抑制するという新しい治療法を開発した[8]. このワクチン療法はOPGの頻回投与によって引き起こされる中和抗体産生によるOPGの効果減弱という問題点を克服することができ，RAや骨粗鬆症における病的骨吸収に対する有効な治療法として今後の臨床応用が注目される.

一方，高柳ら[9]は，活性化Tリンパ球はIFN-γの産生を介して破骨細胞の分化を抑制する実験結果を各種の遺伝子欠損マウスを用いて報告している. その実験成績によると，IFN-γはTリンパ球活性化に伴う骨破壊においてTRAF6（TNF receptor-associated factor 6: RANKL，IL-1，LPSなどのシグナル伝達因子）を標的分子とし，その分解を介してRANKLのシグナル伝達を抑制する機構を有するとしている. したがって，TRAF6の機能や発現を抑制することによって新たな炎症性骨破壊の治療法の確立に道が開けると提唱している[9]. 事実，TRAF6遺伝子欠損マウスは重篤な大理石骨病を呈すること，IFN-γ受容体遺伝子欠損マウスにおいてはコラーゲン誘発性の関節炎が強く発症することなどが報告されている. 更に彼らは，RANKLは破骨細胞前駆細胞におけるc-Fos誘導性のIFN

-β発現を促進し，更にIFN-βはネガティブフィードバックとしてc-Fosの発現を抑制し，破骨細胞分化を阻害する実験結果を報告した[10]. IFN-βのノックアウトマウスは破骨細胞数が増加し骨量が減少するという. このような状況の中，NF-κB，MAPキナーゼおよびc-FosなどのRANKL誘導性の信号伝達が，果たしてどのように破骨細胞の分化と骨吸収機能発現に関与しているかについてはまだまだ謎が多い.

3. OPG遺伝子欠損マウスにおける血清中の可溶性RANKL産生亢進

RANKLのdecoy受容体であるOPGの遺伝子欠損マウスは，破骨細胞の形成が促進し骨吸収が亢進することにより，骨粗鬆症の症状を呈する[11,12]. 更に興味深いことに，OPG欠損マウスは骨吸収の亢進とともに血清中のアルカリホスファターゼ（ALP）活性が上昇し，長管骨において骨形成のパラメーター（骨芽細胞面：ObS%BS）も増加していることが明らかとなった[11]. すなわち，OPG欠損マウスは高い骨代謝共役状態にあることが示唆された. そこで，著者らはOPG欠損マウスに骨吸収阻害薬であるビスホスフォネートを30日間連日投与する実験を行った[13]. その結果，ビスホスフォネート投与は，骨吸収の抑制とともに骨形成も完全に抑制した[13]. この結果は，骨吸収と骨形成が厳格に共役していることを示すものであり，骨代謝共
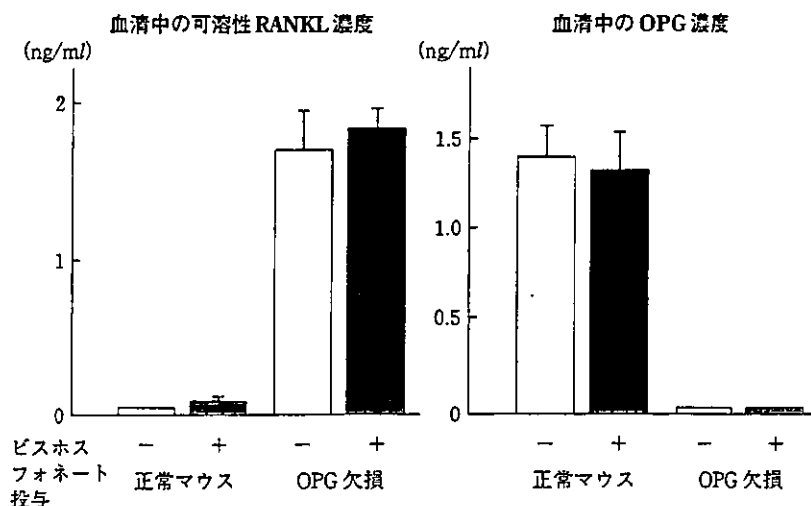
血清中の可溶性RANKL濃度

血清中のOPG濃度

図3 OPG遺伝子欠損マウスにおける血清中の可溶性RANKL産生亢進

役をつかさどる因子(カップリング因子)が実在することを示唆している.

最近,特発性高ホスファターゼ血症(IH)の患者において,OPG遺伝子の変異が発見された[14].興味深いことに,この患者においては,破骨細胞と同様,骨芽細胞が著しく活性化しており,骨形成と骨吸収が活発に行われている組織所見が認められる.また,血清ALP活性(骨形成マーカー)と尿中コラーゲン分解産物であるN-テロペプチド量(骨吸収マーカー)がともにIH患者において高い値を示した[14].

一方,骨Paget病は,破骨細胞の機能異常により限局した骨吸収の亢進が生じ,続いて骨形成が促進する疾患として知られている.最近,遺伝性若年性骨Paget病の原因としてOPG遺伝子の完全な欠損が報告された[15].このOPG欠損患者の血清中にはOPGは検知できないが,興味深いことに可溶性RANKLが高濃度で認められた[15].この実験結果は,高回転型の骨代謝病態に可溶性RANKLの血清レベルでの亢進が関与している可能性を示している.そこで,著者らはOPG欠損マウスにおける血清中の可溶性RANKL濃度を測定した.その結果,正常マウスではほとんど認められない可溶性RANKLがOPG欠損マウスでは高値を呈しており,ビスホスフォネート投与は可溶性RANKLレベルに

は全く影響を与えなかった[13](図3).また,正常マウス血清中にOPGは認められたが,その値はビスホスフォネート投与によって変化しなかった(図3).以上の結果から,可溶性RANKLの産生亢進が,OPG欠損マウスにおける骨形成促進に関与している可能性は否定された.

血清中のOPGは可溶性RANKLと複合体を作ることにより,正常状態では血清中の可溶性RANKLを検知できない可能性が考えられる.そこで,OPGおよびRANKLに対する抗体を用いたELISA法を用いて,OPGとRANKLの複合体を測定した.その結果,OPG-RANKL複合体は正常マウスの血清中には認められなかった[13].この結果は,OPGが欠如することがRANKLの膜型から可溶性への促進(shedding)に作用している可能性を示唆している.以上の実験結果から,OPG欠損マウスの骨組織は高回転型の代謝を呈しており,骨粗鬆症というよりも骨Paget病の病態を示すことが考えられた.可溶性RANKLの存在意義とその由来および遊離メカニズムについては今後の大きな研究課題である.

おわりに

RANKL遺伝子のクローニングにより,破骨細胞の形成を調節する骨芽細胞の役割の詳細が明らかになってきた.更に,RAや歯周疾患の

発症に関与する様々な炎症性サイトカインと RANKLとのシグナル伝達の複雑なクロストークのベールも剥がされつつある．今後，破骨細胞の分化と骨吸収とサイトカインとの関連を証明する更なる研究の発展が期待される．

■文　献

1) Suda T, et al: Modulation of osteoclast differentiation and function by the new members of the tumor necrosis factor receptor and ligand families. Endocr Rev 20: 345-357, 1999.

2) Yasuda H, et al: Osteoclast differentiation factor is a ligand for osteoprotegerin/osteoclastogenesis-inhibitory factor and is identical to TRANCE/RANKL. Proc Natl Acad Sci USA 95: 3597-3602, 1998.

3) Kong YY, et al: OPGL is a key regulator of osteoclastogenesis, lymphocyte development and lymph-node organogenesis. Nature 397: 315-323, 1997.

4) Kotake S, et al: Activated human T cells directly induce osteoclastogenesis from human monocytes: possible role of T cells in bone destruction in rheumatoid arthritis patients. Arthritis Rheum 44: 1003-1012, 2001.

5) Pettit AR, et al: TRANCE/RANKL knockout mice are protected from bone erosion in a serum transfer model of arthritis. Am J Pathol 159: 1689-1699, 2001.

6) Kong YY, et al: Activated T cells regulate bone loss and joint destruction in adjuvant arthritis through osteoprotegerin ligand. Nature 402: 304-309, 1999.

7) Teng YT, et al: Functional human T-cell immunity and osteoprotegerin ligand control alveolar bone destruction in periodontal infection. J Clin Invest 106: R59-67, 2000.

8) Juji T, et al: A novel therapeutic vaccine that prevents pathological bone destruction in models of osteoporosis and RA. J Bone Miner Metab 20: 266-268, 2002.

9) Takayanagi H, et al: T-cell-mediated regulation of osteoclastogenesis by signalling cross-talk between RANKL and IFN-γ. Nature 408: 600-605, 2000.

10) Takayanagi H, et al: RANKL maintains bone homeostasis through c-Fos-dependent induction of interferon-beta. Nature 416: 744-749, 2002.

11) Bucay N, et al: Osteoprotegerin-deficient mice develop early onset osteoporosis and arterial calcification. Genes Dev 12: 1260-1268, 1998.

12) Mizuno A, et al: Severe osteoporosis in mice lacking osteoclastogenesis inhibitory factor/osteoprotegerin. Biochem Biophys Res Commum 247: 610-615, 1998.

13) Nakamura M, et al: Osteoprotegerin regulates bone formation through a coupling mechanism with bone resorption. Endocrinology, 2003. (in press)

14) Hughes AE, et al: Mutations in TNFRSF11A, affecting the signal peptide of RANK, cause familial expansile osteolysis. Nat Genet 24: 45-48, 2000.

15) Whyte MP, et al: Osteoprotegerin deficiency and juvenile Paget's disease. N Engl J Med 347: 175-184, 2002.

骨のリモデリングと骨粗鬆症

中道裕子[*]・高橋直之[**]

abstract

骨組織は吸収と形成を繰り返し，形態と骨量を生涯維持する．この骨リモデリングの制御は，骨吸収を担う破骨細胞と骨形成を担う骨芽細胞との間のコミュニケーションを正と負に調節することで行われる．骨吸収と骨形成は厳格に共役（カップリング）しており，破骨細胞が吸収した部位に骨芽細胞は正確に骨をつくる．骨粗鬆症はこの骨代謝共役が破綻した疾患であり，平衡状態が骨吸収へ偏るために骨量が減少する．骨粗鬆症の病態を理解し治療指針を確立するためには，破骨細胞と骨芽細胞の分化と機能の調節機構および骨代謝共役機構を理解することが重要であろう．

I はじめに

骨吸収を司る破骨細胞は，骨芽細胞（あるいは骨髄間質細胞）の調節機構のもとで単球・マクロファージ系前駆細胞より分化する．近年，破骨細胞の分化および活性化を誘導する因子RANKL（receptor activator of NF-κB ligand）が発見され，骨吸収の調節機構が明らかにされた[1]~[4]．一方，骨形成を司る骨芽細胞は，未分化間葉系細胞から分化する．骨芽細胞の分化は種々のホルモンやサイトカインで制御されるが，そのなかで，BMPs（bone morphogenetic proteins）は最も強力な分化誘導因子である．また，骨芽細胞の分化に必須な転写因子としてRunx2〔runt-related gene 2（Cbfa1）〕が発見された[5],[6]．破骨細胞が吸収した部位に骨芽細胞は正確に骨をつくる．最近の研究より，骨吸収と骨形成は厳格に共役（カップリング）していることが示された．本稿では，破骨細胞と骨芽細胞の分化と機能の調節機構

および骨代謝共役機構を紹介し，骨リモデリング不全としての骨粗鬆症の病態に迫りたい．

II 骨吸収の調節機構

破骨細胞は単球・マクロファージ系前駆細胞より分化，融合して形成される多核細胞である．破骨細胞の分化は，骨芽細胞により厳格に調節されている．骨芽細胞は破骨細胞の分化を誘導する2つのサイトカイン，M-CSF（macrophage colony-stimulating factor）とRANKLを産生する．一方，破骨細胞前駆細胞はM-CSF受容体c-fmsとRANKL受容体RANKを発現する．骨芽細胞によるM-CSFの発現が構成的であるのに対し，RANKLの発現は誘導的である．1,25$(OH)_2D_3$（1,25-dihydroxyvitaminD_3），PTH（parathyroid hormone），PGE2（prostaglandin E_2），IL-11（interleukin-11）などすべての骨吸収促進因子は骨芽細胞のRANKL発現を誘導する[7]．RANKLはTNF（tumor necrosis factor）ファミリ
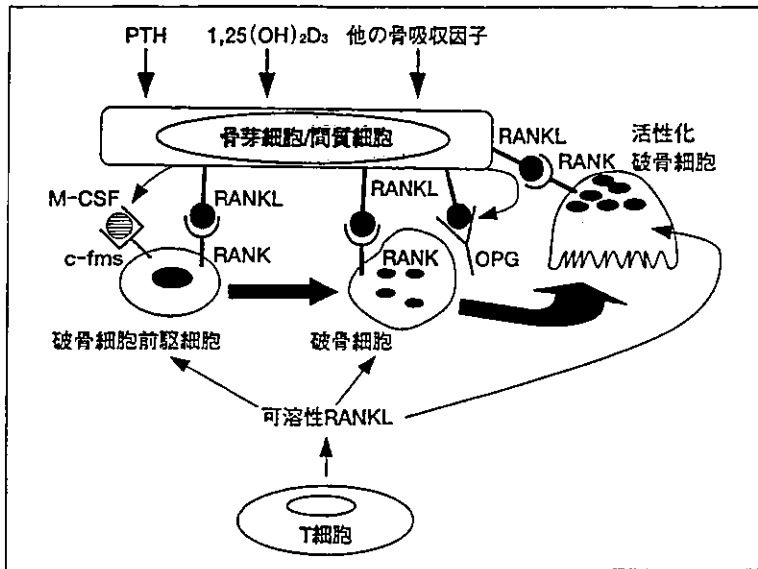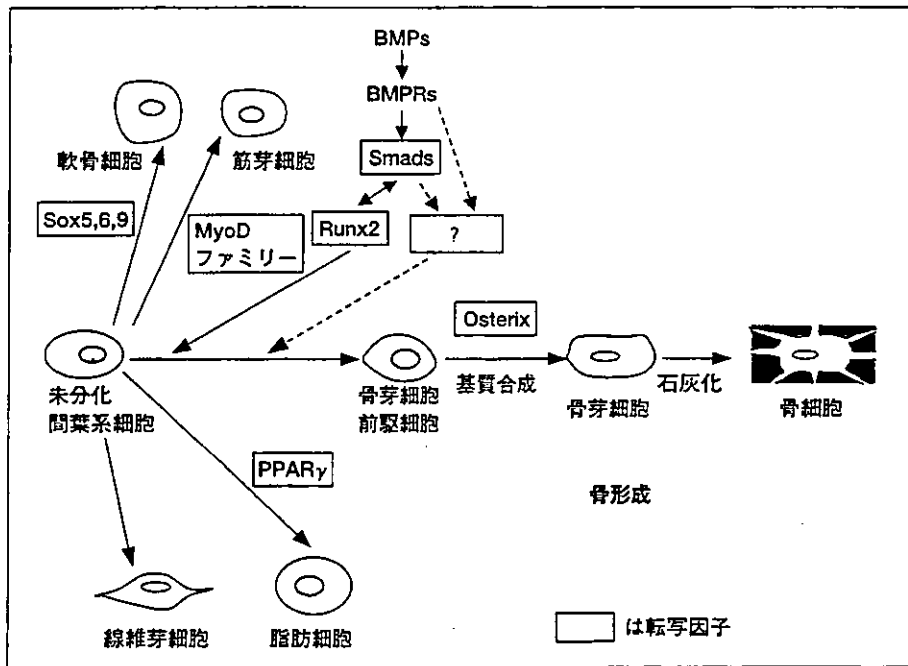

図1
骨吸収を促進する因子

図2
骨芽細胞の分化および機能の調節

ーに属するサイトカインで，骨芽細胞はRANKLを
膜結合因子として発現する．破骨細胞前駆細胞は骨
芽細胞との細胞間接触を介してRANKLを認識し，
M-CSFの存在下で破骨細胞に分化する（図1）．さ
らに，成熟破骨細胞もRANKを発現しており，
RANKシグナルは破骨細胞の骨吸収活性を促進す
る．興味深いことに，骨芽細胞は破骨細胞の形成を
阻害するOPG（osteoprotegerin）を分泌する．
OPGはTNF受容体ファミリーに属するが，膜貫通

ドメインをもたず細胞外に分泌されるタンパクであ
る．OPGはRANKLに特異的に結合しRANKL/
RANKのシグナルを遮断することで骨吸収を抑制す
る[8], [9]．このように，骨芽細胞は破骨細胞に対する
正と負のメディエーターを自ら発現し，骨吸収を制
御する．一方，活性化されたT細胞もRANKLを遊
離型として産生・分泌する．そのため，炎症性骨吸
収にはT細胞由来のRANKLも関与すると考えられ
ている．